International Journal of Mass Spectrometry 306 (2011) 51–56

Contents lists available at ScienceDirect

International Journal of Mass Spectrometry

journal homepage: www.elsevier.com/locate/ijms

Negative ion formation through dissociative electron attachment to GeH_4: Comparative studies with CH_4 and SiH_4

M. Hoshino[a,*], Š. Matejčík[b], Y. Nunes[c], F. Ferreira da Silva[c], P. Limão-Vieira[a,c,**], H. Tanaka[a]

[a] Department of Materials and Life Sciences, Sophia University, Chiyoda-ku, Tokyo 102-8554, Japan
[b] Department of Experimental Physics, Comenius University, Mlynská dolina F2, 84248 Bratislava, Slovakia
[c] Laboratório de Colisões Atómicas e Moleculares, CEFITEC, Departamento de Física, FCT, Universidade Nova de Lisboa, 2829-516 Caparica, Portugal

ARTICLE INFO

Article history:
Received 20 April 2011
Received in revised form 14 June 2011
Accepted 15 June 2011
Available online 20 July 2011

Keywords:
Negative ion formation
Dissociative electron attachment
Germane (GeH_4)
Silane (SiH_4)
Methane (CH_4)
CVD and plasma etching

ABSTRACT

Negative ion formation by low-energy electron impact to germane (GeH_4) has been performed in an electron energy region from 6 to 11 eV with an energy resolution of ~500 meV. Anion efficiency curves of four anions have been measured. Product anions are observed mainly in the 6–11 eV energy region, yielding GeH_x^- (x = 0–3). Comparative studies with methane (CH_4) and silane (SiH_4) are also presented with the most intense signals observed at 14 amu (CH_2^-), 31 amu (SiH_3^-) and 75 amu (GeH_3^-) from CH_4, SiH_4 and GeH_4, respectively. Fragmentation into these negative ions is attributed to resonant dissociative electron attachment processes.

1. Introduction

Electron impact excitation, fragmentation and ionisation of methane (CH_4), silane (SiH_4) and germane (GeH_4) are processes that have invited a lot of research interest owing to their widespread use in chemical vapour deposition (CVD) [1] and plasma etching processes [2]. In particular, fragmentation yielding radicals becomes the most important channel in such processes. Electron impact, unlike photon collisions which are limited by dipole interactions, can excite any dissociative state of a molecule reducing it to fragments. Electron driven reactions are a key mechanism by which radicals and molecular ions are produced in various fields of industrial applications, including aspects related to atmospheric and space sciences [3–6].

The fragmentation of a molecule (XY) by electron (e) impact can proceed in any of the following schematic main pathways:

(i) $e + XY \rightarrow (XY)^* + e \rightarrow X^+ + Y + 2e$, *dissociative ionisation*

(ii) $\rightarrow X^- + Y$, *dissociative electron attachment*

(iii) $\rightarrow X + Y + e$, *non-radiative neutral fragmentation*

(iv) $\rightarrow X^+ + Y^- + e$, *dipolar dissociation*

(v) $\rightarrow X^* + Y + e$,

$\downarrow\rightarrow X + h\nu$ *radiative fragmentation*

Molecular dissociation via electronic excitation forms the core of CVD, whereas ionisation and charge transfer processes also help to maintain the discharge [7]. Inelastic collisions are therefore processes responsible for thermalisation of the secondary electrons in reactors. In silane, for instance, the rapid electron density decay is due to electron attachment processes showing up as an increase in the intensities of negatively charged species. Unfortunately, negative ion formation and the reaction pathways leading to its production are still not yet very well understood. This is evidenced by the scarcity of cross section data for negative ions formed by electron–molecule collisions in comparison to their positive fragment ion formation counterpart (see e.g., Refs. [6,8], and references therein). It is worth noting though a few studies available in the literature which are relevant to the current investigations [9,10]. Recently, experiments on negative ion formation by low-energy electron impact, have been extensively carried out on a number of

* Corresponding author. Tel.: +81 3 3238 4227.
** Corresponding author at: Laboratório de Colisões Atómicas e Moleculares, CEFITEC, Departamento de Física, FCT, Universidade Nova de Lisboa, 2829-516 Caparica, Portugal. Tel.: +351 21 294 78 59; fax: +351 21 294 85 49.
E-mail addresses: masami-h@sophia.ac.jp (M. Hoshino), plimaovieira@fct.unl.pt (P. Limão-Vieira).

1387-3806/$ – see front matter © 2011 Elsevier B.V. All rights reserved.
doi:10.1016/j.ijms.2011.06.009

biologically relevant molecules, see e.g., Refs. [11,12], and in the study of clusters, e.g., Refs. [13,14].

In more closely related studies, critical control of the XH_3 (X = C, Si, Ge) radical production and ion yields in the photochemical vapour deposition of amorphous silicon alloys have been demonstrated to be important for better structural and electronic properties [15]. Note however, that in this photochemical vapour deposition application, radicals and negative ions are produced in dc or rf-glow discharges, and not via electron impact [15]. Joshipura et al. [16] used complex potential calculation methods to study total cross sections, partitioning them into ionisation and electronic excitation cross sections, for electron impact on CH_4, SiH_4 and GeH_4, CF_4, SiF_4 and CCl_4 targets. Photoelectron spectra of CH_4, SiH_4 and GeH_4 have been studied experimentally and the valence ionisation and vibrational excitation results provide useful information on the physical and chemical structures of these molecules [17]. Dirac–Hartree–Fock calculations to establish bond lengths and harmonic frequencies of the ground states of these molecules have been also reported [18]. Elastic collisions of low-energy electrons with CH_4, SiH_4, and GeH_4 have been the subject of several experimental and theoretical investigations [19–21]. These studies have been well reviewed by Bettega et al. [22] and in a separate study they have also investigated the electron impact integral cross sections for the electronic excitation to the $^3T_2$ states [23]. We are aware of only a minor set of studies concerning cross sections for negative ions formation via electron impact on these molecules [24–29]. Tanaka and co-workers have successfully carried out experiments by investigating electron impact on CH_3 neutral radical formation from CH_4 [30], taking particular interest in probing the correlation between production of this neutral radical and its corresponding negative ion (CH_3^-).

In the present work we carried out experimental studies on the negative ion fragment formation of GeH_4 in collisions with 6–11 eV electrons and the results are compared with CH_4 and SiH_4.

2. Experimental procedure

The negative ion formation measurements were performed using an SXP300 quadrupole mass spectrometer (QMS) of the VG Gas Analysis LTD type in the Sophia University, Tokyo, Japan. Details of the experimental technique can be found elsewhere [30], and thus only summarised here highlighting those features particularly relevant to the current study. The spectrometer was attached to a crossed-beam vacuum system. Background pressures were of the order of 1.3×10^{-6} Pa in the absence of target gas beam, and increased to about 6.6×10^{-5} Pa in the presence of the molecular target.

An electron beam produced in a commercial electron gun with typical currents of ~500 nA and energy resolution of ~500 meV (FWHM), are accelerated to the required impact energy crossing the effusive molecular beam emerging through a capillary. The anions formed are focused onto the entrance of the QMS by a single electrostatic Einzel lens system. After mass selection, the anions are detected by a built-in electron multiplier in a pulse counting mode. A weak magnet deflects stray electrons from the detection system. Below 4 eV, the anionic current signal decreased so rapidly that quantitative ion intensities could not be accurately obtained, so we restricted ourselves to energies above 4 eV.

Fig. 1(a)–(c) shows typical mass spectra of negative ions for the XH_4 molecules (X = Ge, Si, and C, respectively). The energy scale was calibrated by observation of the onset on the resonant electron capture for formation of O^- from CO [31]. The time span from ion formation to its detection is in the order of microseconds. For CH_4 measurements, another QMS (Hiden Analytical Ltd. HAL 301 S/2) was used to confirm the reliability of our experimental results. The target gases were obtained from Takachiho Co. with a stated purity of 99.999% for SiH_4 and GeH_4 and 99.0% for CH_4. They were used without additional purification.

3. Results and discussions

The mass spectra in Fig. 1 contain contributions from residual negative ions in the vacuum chamber yielding Cl^- (Fig. 1(a) and (b)). They serve as mass scale calibration but do not interfere with the anions from the XH_4 molecules. H^- detection was not possible due to undistinguishable overlap with stray electrons. Fig. 1 features have been fitted with Gaussian profile curves.

The formation of fragment anions in XH_4 molecules through dissociative electron attachment (DEA) is here mainly restricted to broad features in the 6–14 eV energy region. Figs. 2–4 show the electron energy dependence of the total and the fragment yields for X^-, XH^-, XH_2^- and XH_3^- (X = Ge, Si, and C, respectively) with an electron energy resolution of ~500 meV (FWHM). The most dominant fragment anions are GeH_3^-, SiH_3^- and CH_2^- from GeH_4, SiH_4 and CH_4, respectively. A close inspection to Figs. 2–4, reveals that the total anion yield maximum value is generally speaking the same as for XH^- and XH_2^- fragment anions, and its position follows the sequence $CH_4 \rightarrow SiH_4 \rightarrow GeH_4$ towards lower energies (see Table 1).

The temporary negative ion (TNI) is seen as a quasi-bound state embedded in the autodetachment continuum and is therefore unstable towards the loss of the extra charge. The autodetachment lifetime varies, depending on the nature of the target molecule and on the electron energy. XH_4 are polyatomic molecules, which according to the present measurements belong to a group where autodetachment may occur in a time window shorter than the detection time, resulting in the absence of an observable parent negative ion. However SiH_4^- formation in an ion cyclotron resonance trap has been reported by Haaland [27], over the 6–12 eV energy range, albeit with a very small cross section value ($<8 \times 10^{-21}$ cm^2). Unfortunately in the present experiment we were not able to detect such anion.

Negative ion formation through the capture of a free electron by a XH_4 neutral molecule generates a TNI, $(XH_4)^{\#-}$, that may decompose into:

$$e^- + XH_4 \rightarrow (XH_4)^{\#-} \rightarrow XH_3^- + H \quad (1)$$

$$e^- + XH_4 \rightarrow (XH_4)^{\#-} \rightarrow XH_2^- + 2H \quad (2a)$$

$$e^- + XH_4 \rightarrow (XH_4)^{\#-} \rightarrow XH_2^- + H_2 \quad (2b)$$

while for the decomposition yielding XH^- and X^- in the present energy range (6–14 eV), the structure of their associated neutral counterparts remains unknown. These results are analysed for each molecule as is presented below.

3.1. GeH_4

Four negative fragment anions are observed for GeH_4, i.e., Ge^-, GeH^-, GeH_2^- and GeH_3^-, as shown in Fig. 2. These results were corrected for isotopic contributions from ^{70}Ge, ^{72}Ge, ^{73}Ge, ^{74}Ge and ^{76}Ge (isotope abundance: 20.50%, 27.40%, 7.80%, 36.50%, and 7.80%, respectively). The shape and position of the resonance features (8.8 eV) for GeH^- and GeH_2^- are very similar, which may indicate that these anions may have a common precursor transient anion state. The dominant GeH_3^- ion is shifted to lower energies peaking at 8.26 eV. The Ge^- ion formation is the weakest and shows a broad peak centred around 9.20 eV (Table 1). Most probably all these fragment ions are formed via single negative ion state as the shifts in the peak positions are small and

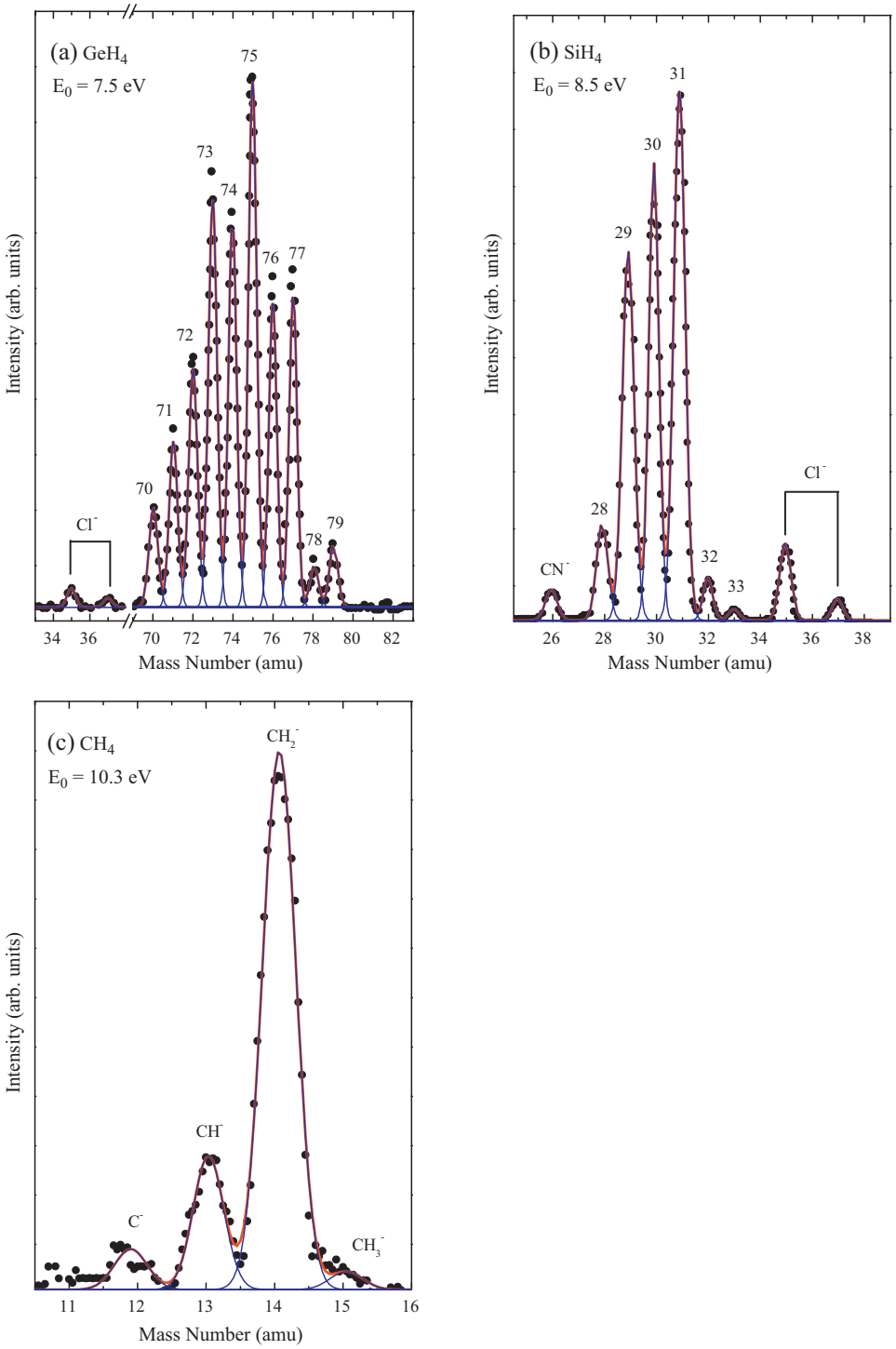

Fig. 1. Typical negative ion mass spectra of XH_4 molecules around the resonant energy (a) GeH_4, (b) SiH_4 and (c) CH_4. The mass spectrum for each sample gas was fitted by the profile of the Gaussian function.

may arise from the dynamics of the dissociation process – interplay of ions formation, autodetachment and the dissociation. The trend in the relative position is similar to those in SiH_4, i.e., the peaks' position shift to lower energies with increasing anion molecular size as $Ge^- \rightarrow GeH^- \rightarrow GeH_2^- \rightarrow GeH_3^-$. There is no such clear trending in the case of CH_4 (Fig. 4), due to the absence of a discernable signal from C^- and especially from CH_3^-, with the exception for $CH^- \rightarrow CH_2^-$. There is no other experimental and theoretical investigation of negative ion formation in this system.

The threshold energy (E_{th}) determined by energy conservation of the DEA reaction (1) is given by:

$$E_{th} = D(XH_3 - H) - EA(XH_3) + E^* \quad (3a)$$

with $D(XH_3 - H)$ the enthalpy of the chemical bond, $EA(XH_3)$ the electron affinity of the (neutral) fragment carrying the extra charge and E^* the total excess energy. Though, as far as standard heats of formation (ΔH_f°) are concerned, Eq. (3a) can be written as:

$$E_{th} = \Delta H_R^\circ = \Delta H_f^\circ(H) + \Delta H_f^\circ(XH_3^-) - \Delta H_f^\circ(XH_4) \quad (3b)$$

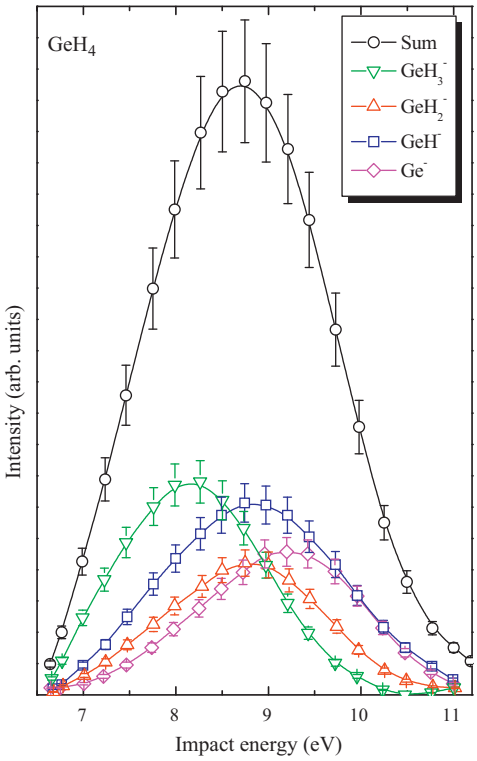

Fig. 2. Ge^-, GeH^-, GeH_2^- and GeH_3^- ion formation results for electron impact from GeH_4. Symbols show the experimental results while the solid lines show the smoothed line of experimental points. Error bars show the statistical uncertainties in these measurements.

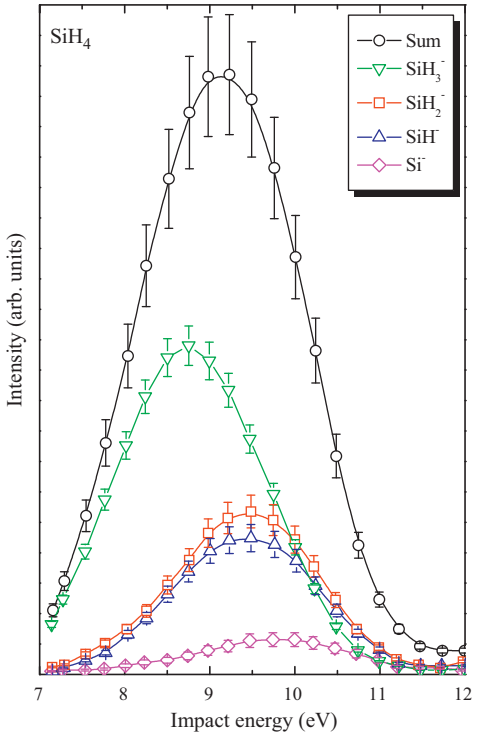

Fig. 3. Si^-, SiH^-, SiH_2^- and SiH_3^- ion formation results for electron impact from SiH_4. Symbols show the experimental results while the solid lines show the smoothed line of experimental points. Error bars show the statistical uncertainties in these measurements.

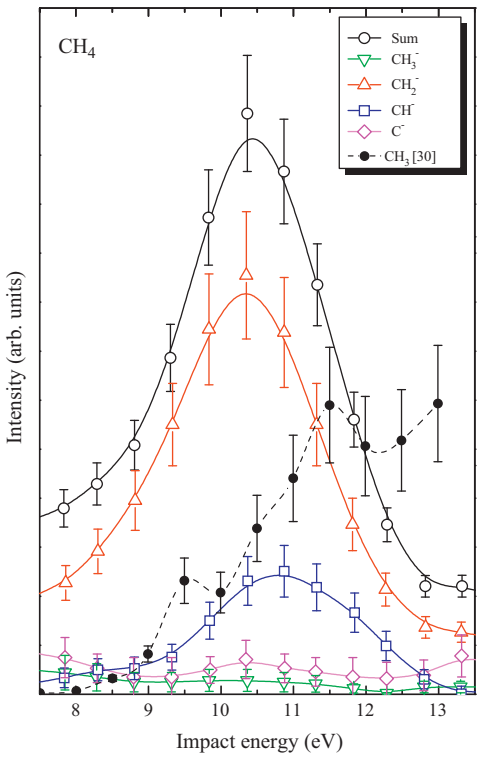

Fig. 4. C CH^-, CH_2^- and CH_3^- ion formation for electron impact from CH_4. Symbols show the experimental results while the solid lines show the smoothed line of experimental points. The recent data on CH_3 radical formation from Makochekanwa et al. [30] is shown for comparison. Error bars show the statistical uncertainties in these measurements.

where ΔH_R° represents the standard heat of reaction (1) with $\Delta H_f^\circ(XH_3^-) = \Delta H_f^\circ(XH_3) - EA(XH_3)$. The threshold energy for reaction (3b) is 2.14 eV, typically below 4 eV [32]. This is not surprising for the case that the anion is formed by simple bond-cleavage and no rearrangement processes in a neutral fragment take place. This is due to the fact that the electron affinity for most radicals (Table 2) is usually less than 4 eV below the bond dissociation energy.

The dissociation channel yielding GeH_2^- formation in the present electron energy region most probably proceeds through reaction (2a). Though, the heats of formation for the radical anion,

Table 1
Peak position maximum for the fragment anions obtained in the present experiment (accuracy ± 10–15%) and reported in previous studies.

Anionic species	Peak position in eV				
	Present work	[24]	[27]	[28]	[29]
GeH_3^-	8.26	–	–	–	–
GeH_2^-	8.75	–	–	–	–
GeH^-	8.74	–	–	–	–
Ge^-	9.20	–	–	–	–
Total anion yield	8.75	–	–	–	–
SiH_3^-	8.75	–	8.5–9.8	8.00	–
SiH_2^-	9.48	–	9.5	8.50	–
SiH^-	9.48	–	9.8–10.7	8.53	–
Si^-	9.99	–	–	9.00	–
H^-	–	–	–	9.00	–
Total anion yield	9.23	–	–	–	–
CH_3^-	–	–	–	–	–
CH_2^-	10.30	10.7	–	–	10.4
CH^-	10.80	11.0	–	–	–
C^-	10.34	–	–	–	–
H^-	–	11.0	–	–	9.8
Total anion yield	10.32	–	–	–	9.9

Table 2
Gas phase standard heats of formation (ΔH_f°) and electron affinities relevant in dissociative electron attachment to XH_4 (X = Ge, Si, C) molecules.

Compound	ΔH_f° (eV)
GeH_4	0.85 [34]
GeH_2^-	1.46 ± 0.20 [33]
GeH_3^-	0.73 ± 0.07 [35]
Ge^-	2.58 ± 0.01 [33]
Compound	**Electron affinity (eV)**
GeH_3	1.61 ± 0.12 [33]
SiH_3	1.406 ± 0.014 [33]
CH_3	0.080 ± 0.030 [33]

$\Delta H_f^\circ(GeH_2^-) = 1.46$ eV [33], the reaction enthalpy becomes ΔH_R° (2a) = 5.04 eV. The appearance energy from Fig. 2 gives a value of ~6.5 eV.

As far as Ge^- formation is concerned, the appearance energy from Fig. 2 gives a value of around 6.5 eV. If we take the silicon analogue and assume the same sort of decomposition reaction from Ref. [28], $e^- + SiH_4 \rightarrow Si^- + H_2 + 2H$, then, $\Delta H_f^\circ(Ge^-) = 2.58$ eV [33] and the reaction enthalpy becomes $\Delta H_R^\circ = 6.16$ eV.

3.2. SiH_4

Fig. 3 shows the anionic yields of Si^-, SiH^-, SiH_2^- and SiH_3^-. Similar to the case of GeH_4, these results were corrected for isotopic contributions from ^{28}Si, ^{29}Si and ^{30}Si (isotope abundance: 92.23%, 4.67%, and 3.10%, respectively) by assuming that negative ion formation does not depend on the isotope. The curves for SiH^- and SiH_2^- peak at a common energy of ~9.5 eV (Table 1) and also show a similar shape that may be an indication common precursor transient anion states. The dominant fragment is SiH_3^- with its peak maximum shifted to lower energies relative to the former fragments, i.e., at 8.75 eV. The Si^- ion formation is the weakest and shows a broad peak centred at around 10 eV.

The present results reproduce qualitatively the measurements of Ebinghaus et al. [25] and Potzinger and Lampe [26] but differ significantly from the results of Haaland [27], who measured the dissociative attachment cross sections of negative fragment ions by using the fourier transform mass spectrometry (FTMS) technique. The differences in Haaland's arise from the fact that (i) he could not observe any Si^- ion formation, (ii) the SiH^- result shows a peak shifted to higher energies, i.e., at 10.5 eV, (iii) the results for SiH_2^- show a peak at somewhat the same energies, i.e., at 9.5 eV, and (iv) SiH_3^- has a peak at higher energies, 9.0 eV. The experimental appearance energies for SiH_2^- and Si^- agree quite well with the data of Srivastava et al. [28].

3.3. CH_4

Like in the two previous cases above, the results for C^-, CH^-, CH_2^- and CH_3^- anions formed from DEA to CH_4, are shown in Fig. 4 as relative cross sections versus electron impact energy. We have performed negative ion measurements from CH_4 using two different sets of QMSs as described in Section 2. The set of results have shown very good agreement. The CH_2^- anion is observed to be the most abundant species produced from the dissociative electron attachment of CH_4 (Fig. 4) and the resonance feature peaks at 10.3 eV (Table 1). CH^- is the next in magnitude, showing a resonance peak at 10.8 eV, and is much weaker and narrower than CH_2^-. Although C^- and CH_3^- anions' production show very weak features in the 7.5–14.0 eV electron energy range and since the error bars for these fragments are of considerable magnitude relative to the signal, we have made no attempt to identify any peak position in Table 1 mainly for the latter. These results agree well with those of Trepka and Neuert [24] in relative intensities, but our results are shifted up in energy by about 1 eV. Though not shown here, all curves for these fragment ions for CH_4 show steep increases in intensities at energies below about 4 eV. We have no explanation for this at the moment.

We have carried out a comparison of the current results for the dissociative electron attachment negative ion production of CH_3^- from CH_4 to the results we have obtained for electron impact fragmentation of CH_4 to produce the CH_3 neutral radical (see Ref. [30]). The contrast between both sets of results can be summarized as follows: (i) whereas the CH_3^- ion profile shown in Fig. 4 is almost flat, production of the CH_3 neutral radical from Ref. [30] is characterised by two peaks at 9.6 and 11.5 eV, i.e., due to electronic excitation of the $^1T_2$ state and transition into the 4*s* Rydberg state, respectively and (ii) CH_2^- production is the most significant decay channel at energies between 7.5 and 13.5 eV, with CH_3^- production being rather insignificant in this energy range. The two almost equal each other outside this range. At about 10.3 eV for instance, CH_2^- production is about four times greater than CH_3^- production. This is in contrast to our study on the neutral fragmentation where we observed that all excited states of CH_4 predominantly result in dissociation via the CH_3 neutral radical channel below 12.5 eV. Even when the CH_2 neutral radical formation channel becomes less significant, the branching ratio CH_3:CH_2 increased from 4:1 at 9.5 eV to 11:1 at 11.5 eV.

3.4. Comparison

Negative ions production in dissociative electron attachment to SiH_4 and CH_4, show that the dominant anions correspond to SiH_3^- and CH_2^-, respectively. It is interesting to note that the intensities of the anionic fragments follow the sequence from the most to the less abundant as $SiH_2^- > SiH^- > Si^-$ and $CH_2^- > CH^- > C^-$ albeit SiH_3^- becomes the strongest in SiH_4 in contrast to CH_3^- in CH_4. Only in the case of GeH_4 where DEA yields GeH^- and GeH_3^-, their intensities are comparable in magnitude. However, common to all three molecules is that the strongest resonance appears at the lowest impact energy in the range studied. The negative ions we have observed can be interpreted as transient anion states of the parent molecules.

4. Conclusion

We carried out experimental studies on dissociative electron attachment to CH_4, SiH_4 and GeH_4 using a quadrupole mass spectrometer. For all three molecules, four negative ions X^-, XH^-, XH_2^- and XH_3^- (X = Ge, Si, and C) have been observed and attributed to transient anion states of the parent molecules. Similarities in fragment ion intensities have been observed between SiH_4 and CH_4, while GeH_4 takes an intermediate position between these two molecules. In the comparison of electron impact fragmentation of CH_4 into negative ions versus neutral radical formation: CH_2^- production was found to be resonant and dominant between 7.5 and 13.5 eV while CH_3^- production was marginal, i.e., in contrast with the observation that CH_4 dissociates exclusively via the CH_3 neutral radical channel below 12.5 eV, showing resonance features at 9.6 and 11.5 eV.

Acknowledgements

PL-V acknowledges his Visiting Professor position at Sophia University, Tokyo, Japan and FFS the Portuguese Foundation for Science and Technology (FCT-MCTES) for post-doctoral grant SFRH/BPD/68979/2010. This work is performed with the support and under the auspices of the NIFS Collaboration Research program

(NIFS08KYAM017). This work forms part of the EU COST Actions CM0601 and CM0805 programmes “ECCL” and “The Chemical Cosmos”, respectively.

References

[1] P. Antoniotti, L. Operti, R. Rabezzana, F. Turco, G.A. Vaglio, F. Grandinetti, J. Mass. Spectrom. 44 (2009) 725.
[2] H. Tanaka, O. Sueoka, Adv. At. Mol. Opt. Phys. 44 (1) (2001), and references therein.
[3] F.G. Celii, P.E. Pehrsson, H.-T. Wang, J.E. Butler, Appl. Phys. Lett. 52 (1988) 2043.
[4] Y. Hirose, Y. Terasawa, Jpn. J. Appl. Phys. 25 (1986) L519.
[5] H. Chatham, D. Hills, R. Robertson, A. Gallagher, J. Chem. Phys. 81 (1984) 1770.
[6] M.A. Ali, Y.K. Kim, W. Hwang, N.M. Weinberger, M.E. Rudd, J. Chem. Phys. 106 (1997) 9602.
[7] H. Tanaka, M. Inokuti, Adv. At. Mol. Opt. Phys. 43 (2000) 1.
[8] S. Feil, P. Sulzer, A. Mauracher, M. Beikircher, N. Wendt, A. Aleem, S. Denifl, F. Zappa, S. Matt-Leubner, A. Bacher, S. Matejcik, M. Probst, P. Scheier, T.D. Märk, J. Phys. Conf. Ser. 86 (2007) 012003.
[9] L. Operti, R. Rabezzana, F. Turco, G.A. Vaglio, Rapid Commun. Mass Spectrom. 19 (2005) 1963.
[10] P. Antoniotti, L. Operti, R. Rabezzana, G.A. Vaglio, A. Guarini, Rapid Commun. Mass Spectrom. 16 (2002) 185.
[11] S. Feil, K. Gluch, S. Matt-Leubner, P. Scheier, J. Limtrakul, M. Probst, H. Deutsch, K. Becker, A. Stamatovic, T.D. Märk, J. Phys. B 37 (2004) 3013.
[12] F. Ferreira da Silva, S. Jaksch, G. Martins, H.M. Dang, M. Dampc, S. Denifl, T.D. Märk, P. Limão-Vieira, J. Liu, S. Yang, A.M. Ellis, P. Scheier, Phys. Chem. Chem. Phys. 11 (2009) 11631.
[13] F. Ferreira da Silva, P. Bartl, S. Denifl, O. Echt, T.D. Märk, P. Scheier, Phys. Chem. Chem. Phys. 11 (2009) 9791.
[14] J. Langer, S. Matt, M. Meinke, P. Tegeder, A. Stamatovic, E. Illenberger, J. Chem. Phys. 113 (2000) 11063.
[15] J. Perrin, Pure Appl. Chem. 62 (1990) 1681.
[16] K.N. Joshipura, M. Vinodkumar, C.G. Limbachiya, B.K. Antony, Phys. Rev. A 69 (2004) 022705.
[17] A.W. Potts, W.C. Prince, Proc. R. Soc. Lond. A 326 (1972) 165.
[18] K.G. Dyall, P.R. Taylor, K. Faegri, Jr., H. Partridge, NASA Report, NASA-CR-187968, N91-18237, p. 43. Also available online at http://ntrs.nasa.gov/archive/nasa/casi.ntrs.nasa.gov/19910008924_1991008924.pdf.
[19] L. Boesten, H. Tanaka, J. Phys. B: At. Mol. Opt. Phys. 24 (1991) 821.
[20] H. Tanaka, L. Boesten, H. Sato, M. Kimura, M.A. Dillon, D. Spence, J. Phys. B: At. Mol. Opt. Phys. 23 (1990) 577.
[21] M.A. Dillon, L. Boesten, H. Tanaka, M. Kimura, H. Sato, J. Phys. B: At. Mol. Opt. Phys. 26 (1993) 3147.
[22] M.H.F. Bettega, M.T. do, N. Varella, M.A.P. Lima, Phys. Rev. A 68 (2003) 012706.
[23] M.H.F. Bettega, L.G. Ferreira, M.A.P. Lima, Phys. Rev. A 57 (1998) 4987.
[24] V.L.V. Trepka, H. Neuert, Z. Naturforsch 19a (1963) 1295.
[25] V.H. Ebinghaus, K. Kraus, W. Müller-Duysing, H. Neuert, Z. Naturforsch 19a (1964) 732.
[26] P. Potzinger, F.W. Lampe, J. Phys. Chem. 73 (1969) 3912.
[27] P. Haaland, J. Chem. Phys. 93 (1990) 4066.
[28] S.K. Srivastava, E. Krishnakumar, A.C. de, A. e Souza, Int. J. Mass Spectrom. Ion Process. 107 (1991) 83.
[29] P. Rawat, V.S. Prabhudesai, M.A. Rahman, N.B. Ram, E. Krishnakumar, Int. J. Mass Spectrom. 277 (2008) 96.
[30] C. Makochekanwa, K. Oguri, R. Suzuki, T. Ishihara, M. Hoshino, M. Kimura, H. Tanaka, Phys. Rev. A 74 (2006) 042704.
[31] R.I. Hall, I. Cadez, C. Schermann, M. Tronc, Phys. Rev. A 15 (1977) 599.
[32] P. Sulzer, A. Mauracher, S. Denifl, M. Probst, T.D. Märk, P. Scheier, E. Illenberger, Int. J. Mass Spectrom. 266 (2007) 138.
[33] NIST Chemistry WebBook. Available from http://webbook.nist.gov/chemistry.
[34] H. Koizumi, J.Z. Dávalos, T. Baer, Chem. Phys. 324 (2006) 385.
[35] M. Decouzon, J.-F. Gal, J. Gayraud, P.-C. Maria, G.-A. Vaglio, P. Volpe, J. Am. Soc. Mass Spectrom. 4 (1993) 54.